

# A Combination of POD-based Model Order Reduction and Thermal Submodeling for Miniaturized Thermoelectric Generator

## INTRODUCTION AND MOTIVATION

Electrically active implants for regenerative therapies (e.g. regeneration of bone tissue or deep brain stimulation for the treatment of motion disorders) are gaining importance within an aging population of industrial nations. To overcome the drawback of the battery-powered implants, energy harvesting technologies were proposed to develop the self-powered medical implants. In this work, we embedded a newly designed thermoelectric generator (TEG) (see Fig. 1) within a realistic human torso model adopted from [1] (see Fig. 2). Furthermore, proper orthogonal decomposition (POD) based model order reduction (MOR) [2] and submodeling methods are combined to enable efficient fast simulation and design optimization of TEG for electrically active implants.

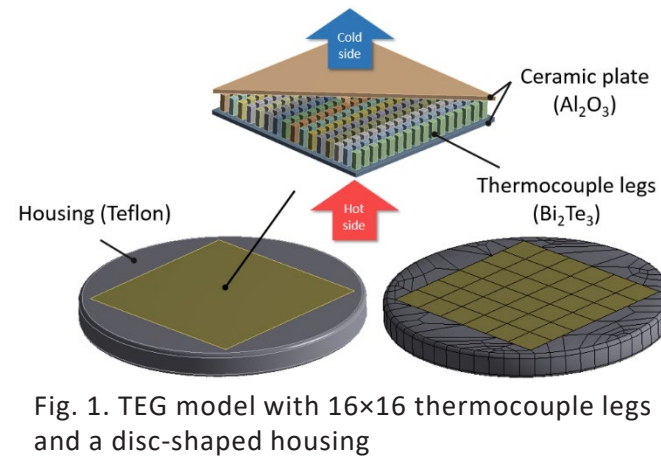


Fig. 1. TEG model with 16x16 thermocouple legs and a disc-shaped housing

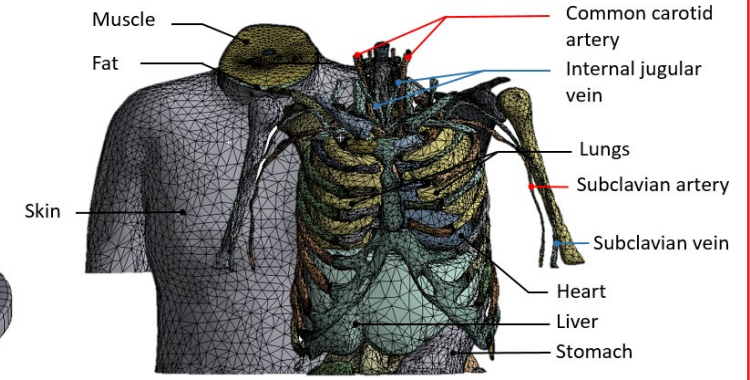


Fig. 2. Human torso model with solid internal organs, skeleton, main vessels, muscle, fat, and skin layers

## MODEL DESCRIPTION

The realistic human torso model is built in ANSYS® Workbench (2019 R1) based on segmented magnetic resonance imaging data. Realistic human tissue material properties are assigned to various tissue sections. We embed TEG in the fat layer of upper-side chest region, where the maximum temperature gradient was observed. The Pennes bio-heat equation [3] is used to describe the heat transfer inside human tissue:

$$\nabla(\kappa\nabla T) + \frac{\rho_b c_b \omega (T_a - T(r, t))}{Q_b} + Q_m = \rho c \frac{\partial T}{\partial t} \quad (1)$$

where  $\rho, c$  and  $\kappa$  are the density, specific heat capacity and thermal conductivity properties of different tissues.  $T$  is the unknown temperature state vector and  $T_a$  is the arterial blood temperature, which is set as constant at 37 °C.  $Q_b$  and  $Q_m$  are the blood perfusion and metabolic heat generation rates applied in muscle, fat, and skin layers, where  $\rho_b, c_b$  describe the thermal properties of blood, and  $\omega$  is a measure of perfusion in different tissues. The external heat transfer effect at the skin surface balance the heat generated inside:

$$q_{sk} = \frac{h_c(T_{skin} - T_{amb})}{q_{conv}} + \frac{\sigma\epsilon(T_{skin}^4 - T_{amb}^4)}{q_{rad}} + \frac{h_e(P_{skin} - \phi P_{sa})}{q_{eva}} \quad (2)$$

where  $q_{conv}$ ,  $q_{rad}$ , and  $q_{eva}$  are the convection, radiation and evaporation heat fluxes normal to the skin surface.  $T_{amb}$  is the environmental temperature and  $T_{skin}$  is the temperature at the skin surface. The details of the variables in equation (2) are given in [4]. After spatial discretization, the model contains 1,045,949 temperature degrees of freedom and can be represented by a nonlinear-input ordinary differential equation system as follows:

$$\sum_N \begin{cases} E \cdot \dot{T}(t) + A \cdot T(t) = \frac{B \cdot u(T(t))}{F(T(t))} \\ y(t) = C \cdot T(t) \end{cases} \quad (3)$$

where  $E, A \in \mathbb{R}^{N \times N}$  are the global heat capacity and heat conductivity matrix.  $F(T(t))$  captures the nonlinearity of the system.  $C \in \mathbb{R}^{q \times N}$  is the user defined output matrix with  $q$  outputs and  $y(t) \in \mathbb{R}^q$  is the output vector.

## POD-BASED MODEL ORDER REDUCTION AND SUBMODELING

Based on the nonlinear-input thermal system (3), a reduced basis (RB) is used as:

$$T(t) = \phi_{pod} \cdot z(t) \quad (4)$$

where  $z(t) \in \mathbb{R}^r, r \ll N$ , is the reduced state vector and RB  $\phi_{pod}$  is obtained through POD method. Singular value decomposition (SVD) is performed on a snapshot matrix  $S \in \mathbb{R}^{N \times n}$ , which contains temperature results in  $n$  time steps:

$$S = [T(t_1), T(t_2), \dots, T(t_n)] = U \Sigma V^T \quad (5)$$

where the columns in  $U = [\phi_1, \phi_2, \dots, \phi_N] \in \mathbb{R}^{N \times N}$  are left-singular vectors of  $S$  and they are mutually orthonormal. The first  $r$  leading singular vectors in  $U$  are truncated for optimal RB space:

$$\phi_{pod} = \text{span}\{\phi_1, \phi_2, \dots, \phi_r\} \in \mathbb{R}^{N \times r} \quad (6)$$

Then, the full-scale system (3) is projected onto the RB  $\phi_{pod}$ :

$$\sum_n \begin{cases} \frac{\phi_{pod}^T E \phi_{pod}}{E_r} \cdot \dot{z}(t) + \frac{\phi_{pod}^T A \phi_{pod}}{\tilde{A}_r} \cdot z(t) = \frac{\phi_{pod}^T F(\phi_{pod} z(t))}{C_r} \\ y(t) = \frac{C \phi_{pod}}{C_r} \cdot z(t) \end{cases} \quad (7)$$

In addition, for providing an efficient TEG design optimization method, submodeling technique is implemented combining with MOR, which separates the simulation of the purely thermal human tissue model and the coupled-domain thermo-electric TEG model. Firstly, a representative TEG model is placed within the thermal human tissue model (see Fig. 3). It is latter reduced and solved. Note that, through equation

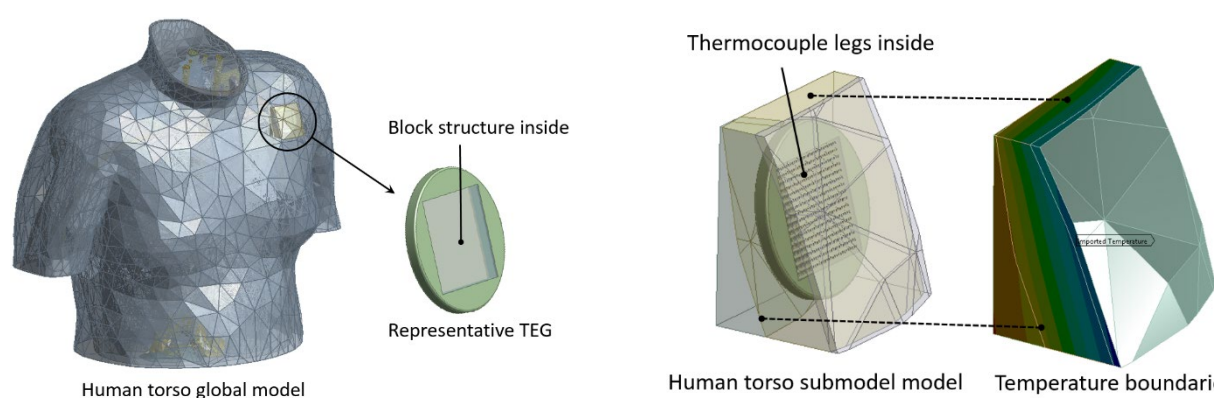


Fig. 3. Global human torso model incorporating the representative TEG with block structure inside

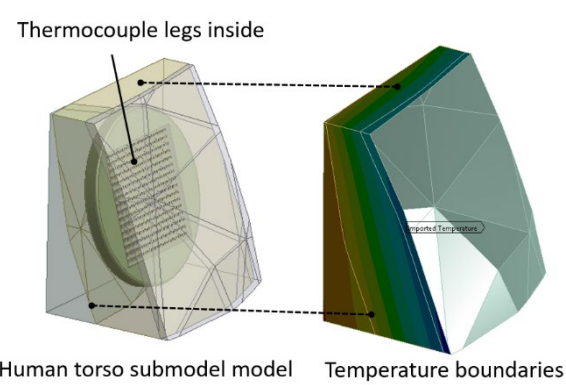


Fig. 4. Human tissue submodel incorporating the detailed TEG, imported temperature boundaries

(4), the full-scale temperature results  $T(t)$  can be easily recovered from the reduced states  $z(t)$  and it is further used as the boundary conditions for the detailed TEG submodel (see Fig. 4). This allows the efficient design alteration and simulation of the TEG in the submodel.

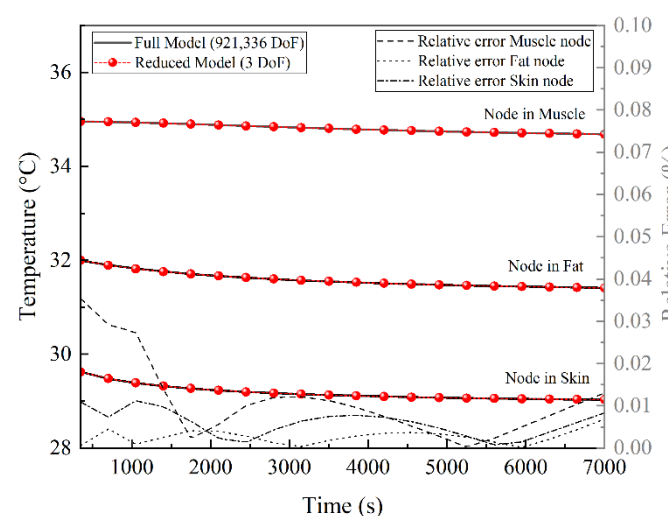


Fig. 5. Comparison of temperature results between full and reduced models (921,336 DoF vs. 3 DoF)

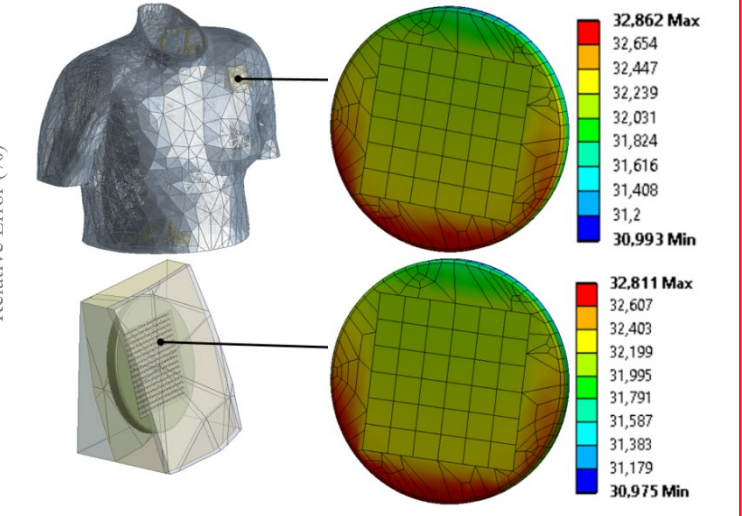


Fig. 6. Detailed TEG simulated separately in global human torso model and submodel

Fig. 5 illustrates that the temperature results obtained from the reduced model are accurate enough for approximating the full-scale temperature results and used as temperature boundary conditions in the submodel. It is observed that the maximum relative error between full and reduced model is 0.035%. Fig. 6 verifies the accuracy of the thermal simulation in the submodel. The temperature results are compared from two detailed TEG models: one was simulated in the global human torso model and the other was simulated in the submodel. The maximum temperature relative error is 0.11%. In the end, the comparison of the computational times are shown in the table below. The generation of the RB in POD is considered as offline effort.

Computational time	Detailed TEG in submodel	Detailed TEG in Global model
MOR	54.6 s	/
Sim. in Submodel	187.73 s	/
Total	242.33 s	1669.56 s

(On HPC with 16x Intel® Xeon® CPU E5-2687W v4 @ 3.00GHz, RAM 324 GB, VGA NVIDIA Tesla M10)

## CONCLUSIONS

- We present a combination of POD-based MOR and submodeling techniques for enabling efficient design optimization of TEG incorporated within realistic human torso model.
- The simulation of the TEG is processed in a relatively small submodel comparing to the global human torso model.
- This approach speeds up the computational time for seeking the temperature gradients on TEG and provides an efficient design optimization process for TEG.

## LITERATURE

- [1] S. Makarov, G. Noetscher, J. Yanamadala, *VHP-Female Datasets*, NEVA Electromagnetics, LLC, vhp-female 2.2 ed. 2015.
- [2] A. Quarteroni et al, "Reduced basis methods for partial differential equations", Springer Switzerland, pp. 115-140, 2016.
- [3] H.H. Pennes, "Analysis of Tissue and Arterial Blood Temperatures in the Resting Human Forearm", *Journal of Applied Physiology*, Vol. 1, Issue 2, pp. 93-122, 1948.
- [4] K. Parsons, "Human thermal environments", 3<sup>rd</sup> ed.: CRC Press, Taylor & Francis, 2014.

